HHS Public Access

Author manuscript

*Dev Dyn*. Author manuscript; available in PMC 2024 April 01.

Published in final edited form as:

*Dev Dyn*. 2023 April ; 252(4): 536–546. doi:10.1002/dvdy.563.

# Characterization of a Novel *Hoxa5eGFP* Mouse Line

**Mu-Hang Li**[1,2], **Julia M. Kuetemeyer**[2], **Alisha R. Yallowitz**[3], **Deneen M. Wellik**[2]

[1]Genetics Training Program, University of Wisconsin-Madison, Madison, WI, United States

[2]Department of Cell and Regenerative Biology, University of Wisconsin-Madison, School of Medicine and Public Health, Madison, WI, United States

[3]Department of Pathology and Laboratory Medicine, Weill Cornell Medicine, New York, NY, United States

## Abstract

**Background:** *Hox* genes encode transcription factors that are important for establishing the body plan. *Hoxa5* is a member of the mammalian *Hox5* paralogous group that regulates the patterning and morphology of the cervical-thoracic region of the axial skeleton. *Hoxa5* also plays crucial functions in lung morphogenesis.

**Results:** We generated a *Hoxa5eGFP* reporter mouse line using CRISPR technology, allowing real-time visualization of *Hoxa5* expression. Hoxa5eGFP recapitulates reported embryonic *Hoxa5* mRNA expression patterns. Specifically, Hoxa5eGFP can be visualized in the developing mouse neural tube, somites, lung, diaphragm, foregut, midgut, among other organs. In the stomach, posteriorly biased Hoxa5eGFP expression correlates with a drastic morphological reduction of the corpus in *Hox5* paralogous mutants. Expression of Hoxa5eGFP in the lung continues in all lung fibroblast populations through postnatal and adult stages.

**Conclusions:** We identified cell types that express *Hoxa5* in postnatal and adult mouse lungs, including various fibroblasts and vascular endothelial cells. This reporter line will be a powerful tool for studies of the function of *Hoxa5* during mouse development, homeostasis, and disease processes.

### Keywords

*Hoxa5* ; mouse reporter; lung mesenchyme; gut development

## 2. Introduction

*Hox* genes code for homeobox-containing transcription factors that are important for patterning during embryonic development and organogenesis.[1–5] There is a total of 39 total *Hox* genes in mammals, collinearly arranged in four distinct chromosomal clusters. They can be further subdivided into 13 groups termed paralogs based on their position within the cluster and similarity in sequence. Genetic loss-of-function analyses have demonstrated

Corresponding Author: Deneen M. Wellik, PhD, Professor and Chair, Department of Cell and Regenerative Biology, University of Wisconsin-Madison, School of Medicine and Public Health, 1111 Highland Avenue, 4405 WIMR II, Madison, WI 53705, 608-262-5491, wellik@wisc.edu.

remarkable redundancy among paralogs. Paralogous *Hox* genes function to pattern the morphology of the axial skeleton and regulate organ formation along the anterior-posterior axis in a region-specific manner.[6,7,7–20]

*Hoxa5* is one of the three members of the *Hox5* paralogous group (*Hoxa5, Hoxb5, Hoxc5*). It encodes a 270-amino-acid protein with a highly conserved DNA-binding homeodomain characteristic of all Hox proteins.[21] Its expression in mice has been previously described. In mouse embryos, *Hoxa5* mRNA expression is first detectable at embryonic day (E) 8.0-8.25 in somite 5-7 and the neural tube.[22] During gut development, dynamic *Hoxa5* expression has been reported in the foregut and midgut mesenchyme from E9.0 through E18.5.[1,22–25] In the skeletal system, *Hoxa5* expression is in vertebral cartilage condensations, anterior rib condensations, and the sternal mesenchyme from E12.5 through E16.5.[23,26–29] *Hoxa5* expression has also been reported in brown adipose tissue from E14.5-E18.5.[28,30] Within the lung, *Hoxa5* is exclusively expressed in the mesenchyme, and not in the epithelium, during development.[19]

The *Hox5* genes function at the anterior limits of their expression boundaries in the developing nervous system (rhombomere 8),[31–33] and also functions to pattern the cervical-thoracic region (cervical vertebra 3 - thoracic vertebra 2).[16,34] These genes are critical for the morphogenesis of the trachea and lung and in the patterning of the stomach. Most *Hoxa5* null (*Hoxa5*$^{-/-}$) animals die perinatally, likely by tracheal collapse and diaphragm defects.[35–39] Lung-specific deletion of *Hoxa5* during postnatal or adult stages leads to distal airways expansion, abnormal pulmonary function, and disruptions of the lung elastin network, phenotypes that are exacerbated in the background of *Hoxb5/Hoxc5* nulls.[40,41] In the gut tube, loss of *Hoxa5* function results in the thinning of the gastric epithelium and delayed development of adult digestive functions.[24,42]

There are some critical outstanding questions in *Hox5* biology that cannot be addressed with the genetic tools currently available. Previous work shows that the *Hox5* paralogous genes (*Hoxa5*, *Hoxb5*, and *Hoxc5*) play a functional role in the mesenchyme of the lung.[40,43] However, lung mesenchymal cell types and lineage relationships remain poorly defined,[44] and little is known about which fibroblast cell type(s) expresses *Hox5* genes in the lung mesenchyme. To address this, we generated a novel *Hoxa5eGFP* reporter line that allows real-time visualization of *Hoxa5* expression. Here we show that expression from this line follows previously reported mRNA expression patterns for *Hoxa5*. Hoxa5eGFP can be detected in the neural tube, lung, diaphragm, foregut, midgut, and other organs at embryonic stages. Expression of Hoxa5eGFP in the lung continues through postnatal and adult stages. Additionally, we are able to isolate and culture lung fibroblasts from *Hoxa5*$^{eGFP/+}$ postnatal and adult animals, which display high *Hoxa5eGFP* expression. This mouse line will be a novel tool for the research community to capture a spatiotemporal expression profile of *Hoxa5* in mice both *in vivo* and *in vitro* and to perform mechanistic studies to dissect *Hoxa5* function.

## 3. Results and Discussion

The *Hoxa5eGFP* allele was generated using Cas/CRISPR technology[45,46] in which the exon 1 of *Hoxa5* is replaced by an in-frame eGFP fusion (Figure 1A) using a similar strategy we have used previously[47]. The *Hoxa5eGFP* allele is a knock-in/knock-out reporter and *Hoxa5eGFP* homozygotes (*Hoxa5*$^{eGFP/eGFP}$) die around birth, recapitulating the described lethality caused by *Hoxa5* loss-of-function.[35] We identified mice carrying the *Hoxa5eGFP* allele by polymerase chain reaction (PCR) genotyping (Figure 1B). F1 offspring from the *Hoxa5*$^{eGFP/+}$ × *Hoxa5*$^{+/+}$ cross follow Mendelian ratios and were used in this study. *Hoxa5*$^{eGFP/+}$ animals are viable and fertile and indistinguishable from *Hoxa5*$^{+/+}$ animals other than Hoxa5eGFP fluorescence.

### 3.1. Hoxa5eGFP expression in whole-mount embryos

*Hoxa5eGFP* expression was initially characterized in freshly dissected whole-mount mouse embryos. Hoxa5eGFP expression is first detected in *Hoxa5*$^{eGFP/+}$ E9.5 embryos in the foregut region (Figure 1C), which will ultimately develop into the lung, liver, gall bladder, pancreas, etc.[48] *Hox5* genes have been shown to express in the phrenic motor column of the hindbrain, and *Hoxa5* mutation is related to reduced and disorganized phrenic motor neurons.[32,37] From E12.5 through later embryonic stages, robust Hoxa5eGFP signal is detected in the hindbrain of the neural tube, the somites, the scapulae, and the stomach (Figure 1D–E). The red arrowhead in Figure 1D indicates the anterior boundary of *Hoxa5* expression at somite 5. *Hoxa5eGFP* expression is not detected in wild-type (WT) littermates at any embryonic stages (Figure 1F).

### 3.2. Hoxa5eGFP localization in the respiratory system during embryogenesis

Strong Hoxa5eGFP signal is also observed in the mouse respiratory system. At E12.5 (Figure 2A–B) and E13.5 (Figure 2C–D), the trachea, bronchi, and lung display robust Hoxa5eGFP signals in the mesenchyme, while no Hoxa5eGFP signal is detected in the epithelium. Notably, we observe high levels of Hoxa5eGFP expression in the diaphragm of E12.5 and E13.5 embryos (Figure 2A,D).

The trachea and the main bronchi transport external air to the distal lung lobes. They are comprised of smooth muscles, fibroblasts, and C-shaped cartilage that regulate the elasticity and rigidity of the airway and prevent the long from collapsing during each breathing cycle.[49] During development, cartilage forms at the ventral side of the trachea and the lateral sides of the main bronchi, adjacent to the smooth muscle layer. SRY-box transcription factor 9 (Sox9) is an early marker for chondroprogenitors during cartilage formation.[50] Immunofluorescence staining shows that Hoxa5eGFP expression and Sox9+ cartilage cells are largely exclusive in the trachea and main bronchi at E16.5, while Hoxa5eGFP is highly overlapping with smooth muscle alpha-actin (SMAα)+ smooth muscles (Figure 2E–F).

### 3.3. Hoxa5eGFP expression and *Hox5* mutant phenotypes in the gastrointestinal tract

Next, we examined the Hoxa5eGFP expression in the embryonic gastrointestinal (GI) tract. Cryosections (Figure 3A–C) and whole-mount images of the gut tube (Figure 3D–E) from *Hoxa5*$^{eGFP/+}$ embryos reveal that *Hoxa5eGFP* is expressed in the mesenchyme of the

stomach, the pancreas (stained with pancreatic and duodenal homeobox 1 (PDX1) antibody, a pancreatic epithelial marker), the duodenum, and the jejunum, with little to no expression in the hindgut or the gut epithelium. As previously reported,[24] a gradient Hoxa5eGFP expression is observed in the stomach, with the strongest expression in the hindstomach, including the corpus and the antrum, with low signal in the forestomach, including the fundus (Figure 3C,D). This expression pattern is maintained from E13.5 to E16.5 (Figure 3D–E). No Hoxa5eGFP expression is detected in the esophagus at any embryonic stage (Figure 2C–F). By comparing to WT littermates, we confirm that the Hoxa5eGFP signal detected in the liver is due to autofluorescence (data not shown).

Although the GI phenotypes of *Hoxa5* null embryos (*Hoxa5*$^{-/-}$) have been reported,[24,42] the effects of losing all the *Hox5* paralogs in this tissue have not been described. Here we show that, at E18.5, the GI tract displays morphological defects in *Hox5* triple mutant (*Hoxa5*$^{-/-}$*;Hoxb5*$^{-/-}$*;Hoxc5*$^{-/-}$ or *Hox5aabbcc*) embryos when compared to controls (Figure 3F–I). Specifically, the corpus of the *Hox5* null mutant (*Hox5aabbcc*) exhibits a significant size reduction, with the fundus and antrum displaying relatively normal morphology (Figure 3F–G). Additionally, loss of all *Hox5* alleles leads to a shortened length of the small intestine, while the appearance of the cecum and the length of the large intestine are not noticeably altered (Figure 3H–I). These phenotypes are consistent with the gradient expression of Hoxa5eGFP in the stomach and small intestine expression of *Hox5* genes in the mouse.[25] These data demonstrate a redundant role for *Hox5* paralogs in gut formation.

### 3.4. Hoxa5eGFP expression in the postnatal and adult lung

To characterize *Hoxa5* expression in the lung, we performed immunofluorescence (IF) in postnatal and adult *Hoxa5*$^{eGFP/+}$ lung cryosections with antibodies against GFP and lung cell-type specific antigens to identify cell types that are Hoxa5eGFP-positive. IF reveals that Hoxa5eGFP is not expressed in T1α+ alveolar epithelial cell (AEC) type I cells, surfactant protein C (SPC)+ AEC type II cells, or Wilms' tumor 1 (WT1)+ mesothelial cells in either postnatal (Figure 4A,B,G) or adult lungs (Figure 5A,B,F). In contrast, in the postnatal lung, a large number of SMAα+ myofibroblasts, adipocyte differentiation-related protein (ADRP) + lipofibroblasts, and platelet-derived growth factor receptor alpha (PDGFRα)+ fibroblasts show Hoxa5eGFP expression (Figure 4C,D,E, **white arrowheads)**. Similarly, ADRP+ lipofibroblasts and PDGFRα+ fibroblasts were largely overlapping with Hoxa5eGFP+ cells in the adult *Hoxa5*$^{eGFP/+}$ lung (Figure 5C,D, **white arrowheads)**. Interestingly, co-staining of mouse GFP and ETS-related gene (ERG, a vascular endothelial marker) antibodies reveals Hoxa5eGFP expression in both postnatal (Figure 4F, **white arrowheads)** and adult (Figure 5E, **white arrowheads)** lung vascular endothelial cells. No Hoxa5eGFP fluorescence is detected in the airway epithelium (Figure 4F and Figure 5A,E). These results are consistent with the *Hoxa5* expression profile in single-cell RNA-sequencing data from a postnatal day 7 mouse lung reported in LungGENS (https://research.cchmc.org/pbge/lunggens/genequery_PN7.html?geneid=hoxa5).[51–53]

Next, we isolated lung fibroblasts from postnatal and adult *Hoxa5*$^{+/+}$ as well as *Hoxa5*$^{eGFP/+}$ mice via enzymatic digestion and cultured them *in vitro*. At passage 0, most fibroblasts isolated from postnatal and adult *Hoxa5*$^{eGFP/+}$ lungs are Hoxa5eGFP-positive, while no

Hoxa5eGFP signal is detected in WT fibroblasts (Figure 6A–C). This high Hoxa5eGFP expression percentage is maintained through later passages and, using flow cytometry, nearly 95% of live, adult *Hoxa5*$^{eGFP/+}$ fibroblasts are Hoxa5eGFP-positive at passage 8 (Figure 6D).

In summary, we generated and characterized a novel Hoxa5eGFP reporter mouse line that closely recapitulates the previously reported *Hoxa5* mRNA expression in the mouse respiratory tract, GI tract, neural tube and skeleton, demonstrating that it is a fidelitous reporter line. We also identified cell types that express *Hoxa5* in postnatal and adult mouse lungs that include various fibroblasts and vascular endothelial cells. Finally, this reporter line will be a helpful tool for monitoring *Hoxa5* cellular localization *in vivo* and isolating *Hoxa5*-expressing cells *in vitro* to interrogate the function of *Hoxa5* during mouse development, homeostasis, and disease.

## 4. Experimental Procedures

### 4.1. Generation of *Hoxa5eGFP* mice and *Hox5* null mutants

The Hoxa5eGFP line was produced by Jackson Laboratories with an eGFP construct inserted as an in-frame fusion just after the start codon in exon 1 of *Hoxa5*, resulting in the deletion of most of exon 1. The eGFP construct is followed by a bovine growth hormone polyadenylation (bGH-PolyA) signal terminator, such that the *Hoxa5* locus is knocked out and eGFP will function as a real-time reporter of the Hoxa5 protein.

The reporter line was generated in the C57BL/6J mouse background. Oligonucleotides used for crRNA were as follows: Up_crRNA: atttgggtgcctacgtagga; Down_crRNA: tctgatccacgcgtccgtgg. The founder line was identified by PCR analysis by using the following primers: Homology Arm Spanning Assay--Hoxa5_eGFP_HA-LHAF: atcggctctggctactgaaa; Hoxa5_eGFP_HA-RHAR: gttggtgtgaagccacaatg (WT amplicon = 4273 bp; eGFP KI amplicon = 4639 bp). Left Homology Arm Assay--Hoxa5_eGFP_HA-LHAF: atcggctctggctactgaaa; Hoxa5_eGFP_LHAR: gaacttcagggtcagcttgc (eGFP KI amplicon = 1720 bp). Right Homology Arm Assay--Hoxa5_eGFP_RHAF: acgtaaacggccacaagttc; Hoxa5_eGFP_HA-RHAR: gttggtgtgaagccacaatg (eGFP KI amplicon = 2996 bp). Donor Plasmid Backbone Assay -- (detects random integrations of the donor plasmid, all N1s were confirmed to be negative for this assay): pUC57_F: ttgggtaacgccagggttttc; Hoxa5_eGFP_LHAR: gaacttcagggtcagcttgc (Tg/Random Insertion amplicon = 1742 bp). Long-range PCR products from the homology arm, left homology arm, and right homology arm assays were sequenced with the primers used for amplification as well as: GenoF: gggatacaaagccggggaaa; GenoR: caccccattttcctccctcc; Hoxa5_eGFP_SRF: acgtaaacggccacaagttc; Hoxa5_eGFP_SRR: tgctcaggtagtggttgtcg.

Three N1 generation mice (2 males and 1 female) carrying the *Hoxa5eGFP* allele were produced from the founder line and their offspring used in this study were found to be indistinguishable in fluorescence. Primers used for PCR to distinguish *Hoxa5*$^{+/+}$ or *Hoxa5*$^{eGFP/+}$ offspring were as follows: WT Forward: cgcccgctcagccccagatctacc; GFP Forward: cgacaaccactacctgagca; Shared Reverse: ctgctgcagtaattgggaggaa (WT amplicon = 235 bp; eGFP amplicon = 519 bp).

The generation of *Hox5* null mutant (*Hoxa5*$^{-/-}$; *Hoxb5*$^{-/-}$;*Hoxc5*$^{-/-}$ or *Hox5aabbcc*) has been previously reported.[16]

### 4.2. Whole-mount embryo and GI tract imaging

Whole-mount *Hoxa5*$^{eGFP/+}$ embryo in Figure 1 and GI tract in Figure 3D–E were dissected out at various stages, washed in 1× PBS solution, and immediately imaged on a ZEISS Axio Zoom V16 Axiocam 506 Camera. Whole-mount stomachs and intestines of control and *Hox5aabbcc* mutants in Figure 3F–I were imaged on a Leica MZ125 Dissecting Microscope.

### 4.3. Cryosection and immunostaining

*Hoxa5*$^{+/+}$ and *Hoxa5*$^{eGFP/+}$ mouse embryos, postnatal and adult lungs were washed in 1× PBS solution, fixed in 4% PFA at 4°C, moved to 30% sucrose (in 1× PBS) at 4°C, embedded in O.C.T (Fisher Sci., #23730571) for cryosection. The specimens were sectioned on a Leica CM3050 S Cryostat (embryos: 14 μm/section; lungs: 7 μm/section) at −18°C.

For immunostaining, sections were baked at 65°C for 10 minutes, blocked in 5% donkey serum (Sigma, #D9663) at room temperature for 1 hour, incubated in primary antibodies at 4°C overnight, incubated in secondary antibodies at room temperature for 2 hours, incubated with 5 μg/ml DAPI (Thermo Sci., #62248) at room temperature for 10 minutes and mounted using ProLong Gold Mountant (Fisher Sci., #P36930). The full primary antibody list is provided in Table 1. Embryonic sections in Figure 2 and Figure 3A–C were imaged on a Keyence BZ-X800 Microscope and processed via the Keyence BZ-X800 Analyzer Software. Lung sections in Figure 4 and Figure 5 were captured on a Leica SP8 3X STED Confocal/ Super-Resolution Microscope at the University of Wisconsin Optical Imaging Core and further analyzed via ImageJ 2.0.0.

### 4.4. Lung Fibroblast Culture, Imaging and Flow Cytometry

Lung fibroblasts in Figure 6A–C were isolated and cultured as previously described,[41] imaged and processed using the Incucyte® S3 Live-Cell Analysis System (Essen BioScience). For flow cytometry data in Figure 6D, *Hoxa5*$^{eGFP/+}$ adult lung fibroblasts were cultured to passaged 8 and analyzed on the Sony MA900 Multi-Application Cell Sorter at the University of Wisconsin Carbone Cancer Center Flow Cytometry Laboratory.

## Acknowledgments

The authors thank the Jackson Laboratory for generating the *Hoxa5eGFP* mouse line and Aubrey E. McDermott and Angelo Madruga for their assistance with mouse genotyping. The authors acknowledge the Biomedical Research Model Services at the School of Medicine and Public Health at the University of Wisconsin, the University of Wisconsin Optical Imaging Core, and the University of Wisconsin Carbone Cancer Center Flow Cytometry Laboratory, supported by P30 CA014520, for use of their facilities and services. The authors acknowledge the LungMAP project funded by the National Heart, Lung, and Blood Institute (NHLBI) 24HL148865 for the reference of its data. This work was supported by the NHLBI R01-HL137364 to DMW.

**5. Grant Sponsor and Number:**

This work was supported by the National Institutes of Health (National Heart, Lung, and Blood Institute (NHLBI) R01-HL137364) to Deneen M. Wellik.

## 6. References


1. Dony C, Gruss P. Specific expression of the Hox 1.3 homeo box gene in murine embryonic structures originating from or induced by the mesoderm. EMBO J. 1987;6(10):2965–2975. [PubMed: 2891502]
2. Duboule D, Dollé P. The structural and functional organization of the murine HOX gene family resembles that of Drosophila homeotic genes. EMBO J. 1989;8(5):1497–1505. Accessed April 27, 2022. https://www.ncbi.nlm.nih.gov/pmc/articles/PMC400980/ [PubMed: 2569969]
3. Krumlauf R Hox genes in vertebrate development. Cell. 1994;78(2):191–201. 10.1016/0092-8674(94)90290-9 [PubMed: 7913880]
4. Duboule D The rise and fall of Hox gene clusters. Development. 2007;134(14):2549–2560. 10.1242/dev.001065 [PubMed: 17553908]
5. Mallo M, Wellik DM, Deschamps J. Hox genes and regional patterning of the vertebrate body plan. Dev Biol. 2010;344(1):7–15. 10.1016/j.ydbio.2010.04.024 [PubMed: 20435029]
6. Davis AP, Witte DP, Hsieh-Li HM, Potter SS, Capecchi MR. Absence of radius and ulna in mice lacking hoxa-11 and hoxd-11. Nature. 1995;375(6534):791–795. 10.1038/375791a0 [PubMed: 7596412]
7. Fromental-Ramain C, Warot X, Lakkaraju S, et al. Specific and redundant functions of the paralogous Hoxa-9 and Hoxd-9 genes in forelimb and axial skeleton patterning. Dev Camb Engl. 1996;122(2):461–472. 10.1242/dev.122.2.461
8. Fromental-Ramain C, Warot X, Messadecq N, LeMeur M, Dollé P, Chambon P. Hoxa-13 and Hoxd-13 play a crucial role in the patterning of the limb autopod. Dev Camb Engl. 1996;122(10):2997–3011. 10.1242/dev.122.10.2997
9. Chen F, Capecchi MR. Targeted Mutations in Hoxa-9 and Hoxb-9 Reveal Synergistic Interactions. Dev Biol. 1997;181(2):186–196. 10.1006/dbio.1996.8440 [PubMed: 9013929]
10. Manley NR, Capecchi MR. Hox group 3 paralogs regulate the development and migration of the thymus, thyroid, and parathyroid glands. Dev Biol. 1998;195(1):1–15. 10.1006/dbio.1997.8827 [PubMed: 9520319]
11. Rossel M, Capecchi MR. Mice mutant for both Hoxa1 and Hoxb1 show extensive remodeling of the hindbrain and defects in craniofacial development. Dev Camb Engl. 1999;126(22):5027–5040. 10.1242/dev.126.22.5027
12. Chen F, Capecchi MR. Paralogous mouse Hox genes, Hoxa9, Hoxb9, and Hoxd9, function together to control development of the mammary gland in response to pregnancy. Proc Natl Acad Sci. 1999;96(2):541–546. 10.1073/pnas.96.2.541 [PubMed: 9892669]
13. van den Akker E, Fromental-Ramain C, de Graaff W, et al. Axial skeletal patterning in mice lacking all paralogous group 8 Hox genes. Dev Camb Engl. 2001;128(10):1911–1921. 10.1242/dev.128.10.1911
14. Wellik DM, Hawkes PJ, Capecchi MR. Hox11 paralogous genes are essential for metanephric kidney induction. Genes Dev. 2002;16(11):1423–1432. 10.1101/gad.993302 [PubMed: 12050119]
15. Wellik DM, Capecchi MR. Hox10 and Hox11 genes are required to globally pattern the mammalian skeleton. Science. 2003;301(5631):363–367. 10.1126/science.1085672 [PubMed: 12869760]
16. McIntyre DC, Rakshit S, Yallowitz AR, et al. Hox patterning of the vertebrate rib cage. Development. 2007;134(16):2981–2989. 10.1242/dev.007567 [PubMed: 17626057]
17. Xu B, Wellik DM. Axial Hox9 activity establishes the posterior field in the developing forelimb. Proc Natl Acad Sci U S A. 2011;108(12):4888–4891. 10.1073/pnas.1018161108 [PubMed: 21383175]
18. Xu B, Hrycaj SM, McIntyre DC, et al. Hox5 interacts with Plzf to restrict Shh expression in the developing forelimb. Proc Natl Acad Sci. 2013;110(48):19438–19443. 10.1073/pnas.1315075110 [PubMed: 24218595]
19. Hrycaj SM, Dye BR, Baker NC, et al. Hox5 Genes Regulate the Wnt2/2b-Bmp4-Signaling Axis during Lung Development. Cell Rep. 2015;12(6):903–912. 10.1016/j.celrep.2015.07.020 [PubMed: 26235626]

20. Larsen BM, Hrycaj SM, Newman M, Li Y, Wellik DM. Mesenchymal Hox6 function is required for mouse pancreatic endocrine cell differentiation. Dev Camb Engl. 2015;142(22):3859–3868. 10.1242/dev.126888
21. Odenwald WF, Taylor CF, Palmer-Hill FJ, Friedrich V, Tani M, Lazzarini RA. Expression of a homeo domain protein in noncontact-inhibited cultured cells and postmitotic neurons. Genes Dev. 1987;1(5):482–496. 10.1101/gad.1.5.482 [PubMed: 2890554]
22. Larochelle C, Tremblay M, Bernier D, Aubin J, Jeannotte L. Multiple cis-acting regulatory regions are required for restricted spatio-temporal Hoxa5 gene expression. Dev Dyn. 1999;214(2):127–140. 10.1002/(SICI)1097-0177(199902)214:2<127::AID-AJA3>3.0.CO;2-F [PubMed: 10030592]
23. Gaunt SJ, Coletta PL, Pravtcheva D, Sharpe PT. Mouse Hox-3.4: homeobox sequence and embryonic expression patterns compared with other members of the Hox gene network. Development. 1990;109(2):329–339. 10.1242/dev.109.2.329 [PubMed: 1976088]
24. Aubin J, Déry U, Lemieux M, Chailler P, Jeannotte L. Stomach regional specification requires Hoxa5-driven mesenchymal-epithelial signaling. Development. 2002;129(17):4075–4087. 10.1242/dev.129.17.4075 [PubMed: 12163410]
25. Kawazoe Y, Sekimoto T, Araki M, Takagi K, Araki K, Yamamura K ichi. Region-specific gastrointestinal Hox code during murine embryonal gut development. Dev Growth Differ. 2002;44(1):77–84. 10.1046/j.1440-169x.2002.00623.x [PubMed: 11869294]
26. Dressler GR, Gruss P. Anterior boundaries of Hox gene expression in mesoderm-derived structures correlate with the linear gene order along the chromosome. Differ Res Biol Divers. 1989;41(3):193–201. 10.1111/j.1432-0436.1989.tb00747.x
27. Aubin J, Lemieux M, Tremblay M, Behringer RR, Jeannotte L. Transcriptional interferences at the Hoxa4/Hoxa5 locus: Importance of correct Hhoxa5 expression for the proper specification of the axial skeleton. Dev Dyn. 1998;212(1):141–156. 10.1002/(SICI)1097-0177(199805)212:1<141::AID-AJA13>3.0.CO;2-A [PubMed: 9603431]
28. Holzman MA, Bergmann JM, Feldman M, Landry-Truchon K, Jeannotte L, Mansfield JH. HOXA5 protein expression and genetic fate mapping show lineage restriction in the developing musculoskeletal system. Int J Dev Biol. 2018;62(11-12):785–796. 10.1387/ijdb.180214jm [PubMed: 30604848]
29. Mitchel K, Bergmann JM, Brent AE, et al. Hoxa5 Activity Across the Lateral Somitic Frontier Regulates Development of the Mouse Sternum. Front Cell Dev Biol. 2022;10. Accessed May 20, 2022. 10.3389/fcell.2022.806545
30. Holzman MA, Ryckman A, Finkelstein TM, et al. HOXA5 Participates in Brown Adipose Tissue and Epaxial Skeletal Muscle Patterning and in Brown Adipocyte Differentiation. Front Cell Dev Biol. 2021;9. Accessed August 29, 2022. 10.3389/fcell.2021.632303
31. Holland PW, Hogan BL. Spatially restricted patterns of expression of the homeobox-containing gene Hox 2.1. during mouse embryogenesis. Development. 1988;102(1):159–174. 10.1242/dev.102.1.159 [PubMed: 2458220]
32. Philippidou P, Dasen JS. Hox Genes: Choreographers in Neural Development, Architects of Circuit Organization. Neuron. 2013;80(1):12–34. 10.1016/j.neuron.2013.09.020 [PubMed: 24094100]
33. Kam MKM, Lui VCH. Roles of Hoxb5 in the development of vagal and trunk neural crest cells. Dev Growth Differ. 2015;57(2):158–168. 10.1111/dgd.12199 [PubMed: 25703667]
34. Wellik DM. Hox patterning of the vertebrate axial skeleton. Dev Dyn Off Publ Am Assoc Anat. 2007;236(9):2454–2463. 10.1002/dvdy.21286
35. Aubin J, Lemieux M, Tremblay M, Bérard J, Jeannotte L. Early Postnatal Lethality in Hoxa-5 Mutant Mice Is Attributable to Respiratory Tract Defects. Dev Biol. 1997;192(2):432–445. 10.1006/dbio.1997.8746 [PubMed: 9441679]
36. Mandeville I, Aubin J, LeBlanc M, et al. Impact of the Loss of Hoxa5 Function on Lung Alveogenesis. Am J Pathol. 2006;169(4):1312–1327. 10.2353/ajpath.2006.051333 [PubMed: 17003488]
37. Philippidou P, Walsh CM, Aubin J, Jeannotte L, Dasen JS. Sustained Hox5 gene activity is required for respiratory motor neuron development. Nat Neurosci. 2012;15(12):1636–1644. 10.1038/nn.3242 [PubMed: 23103965]

38. Boucherat O, Montaron S, Bérubé-Simard FA, et al. Partial functional redundancy between Hoxa5 and Hoxb5 paralog genes during lung morphogenesis. Am J Physiol-Lung Cell Mol Physiol. 2013;304(12):L817–L830. 10.1152/ajplung.00006.2013 [PubMed: 23585229]
39. Landry-Truchon K, Houde N, Boucherat O, et al. HOXA5 plays tissue-specific roles in the developing respiratory system. Dev Camb Engl. 2017;144(19):3547–3561. 10.1242/dev.152686
40. Hrycaj SM, Marty-Santos L, Cebrian C, et al. Hox5 genes direct elastin network formation during alveologenesis by regulating myofibroblast adhesion. Proc Natl Acad Sci. 2018;115(45):E10605–E10614. 10.1073/pnas.1807067115 [PubMed: 30348760]
41. Li MH, Marty-Santos LM, van Ginkel PR, et al. The Lung Elastin Matrix Undergoes Rapid Degradation Upon Adult Loss of Hox5 Function. Front Cell Dev Biol. 2021;9:3057. 10.3389/fcell.2021.767454
42. Aubin J, Chailler P, Ménard D, Jeannotte L. Loss of Hoxa5 gene function in mice perturbs intestinal maturation. Am J Physiol-Cell Physiol. 1999;277(5):C965–C973. 10.1152/ajpcell.1999.277.5.C965
43. Hrycaj SM, Marty-Santos L, Rasky AJ, Lukacs NW, Wellik DM. Loss of Hox5 function results in myofibroblast mislocalization and distal lung matrix defects during postnatal development. Sci CHINA Life Sci. 2018;61(9):1030–1038. 10.1007/s11427-017-9290-1 [PubMed: 29752580]
44. Riccetti M, Gokey JJ, Aronow B, Perl AKT. The elephant in the lung: Integrating lineage-tracing, molecular markers, and single cell sequencing data to identify distinct fibroblast populations during lung development and regeneration. Matrix Biol. 2020;91-92:51–74. 10.1016/j.matbio.2020.05.002 [PubMed: 32442602]
45. Yang H, Wang H, Jaenisch R. Generating genetically modified mice using CRISPR/Cas-mediated genome engineering. Nat Protoc. 2014;9(8):1956–1969. 10.1038/nprot.2014.134 [PubMed: 25058643]
46. Qin W, Kutny PM, Maser RS, et al. Generating Mouse Models Using CRISPR-Cas9-Mediated Genome Editing. Curr Protoc Mouse Biol. 2016;6(1):39–66. 10.1002/9780470942390.mo150178 [PubMed: 26928663]
47. Nelson LT, Rakshit S, Sun H, Wellik DM. Generation and expression of a Hoxa11eGFP targeted allele in mice. Dev Dyn. 2008;237(11):3410–3416. 10.1002/dvdy.21756 [PubMed: 18942146]
48. Method AM, Wells JM. Chapter 30 - Patterning the Embryonic Endoderm into Presumptive Organ Domains. In: Moody SA, ed. Principles of Developmental Genetics (Second Edition). Oxford: Academic Press; 2015:545–564. 10.1016/B978-0-12-405945-0.00030-2
49. Kishimoto K, Morimoto M. Mammalian tracheal development and reconstruction: insights from in vivo and in vitro studies. Development. 2021;148(13):dev198192. 10.1242/dev.198192 [PubMed: 34228796]
50. Bi W, Deng JM, Zhang Z, Behringer RR, de Crombrugghe B. Sox9 is required for cartilage formation. Nat Genet. 1999;22(1):85–89. 10.1038/8792 [PubMed: 10319868]
51. Du Y, Guo M, Whitsett JA, Xu Y. 'LungGENS': a web-based tool for mapping single-cell gene expression in the developing lung. Thorax. 2015;70(11):1092–1094. 10.1136/thoraxjnl-2015-207035 [PubMed: 26130332]
52. Du Y, Kitzmiller JA, Sridharan A, et al. Lung Gene Expression Analysis (LGEA): an integrative web portal for comprehensive gene expression data analysis in lung development. Thorax. 2017;72(5):481–484. 10.1136/thoraxjnl-2016-209598 [PubMed: 28070014]
53. Du Y, Ouyang W, Kitzmiller JA, et al. Lung Gene Expression Analysis Web Portal Version 3: Lung-at-a-Glance. Am J Respir Cell Mol Biol. 2021;64(1):146–149. 10.1165/rcmb.2020-0308LE [PubMed: 33385216]

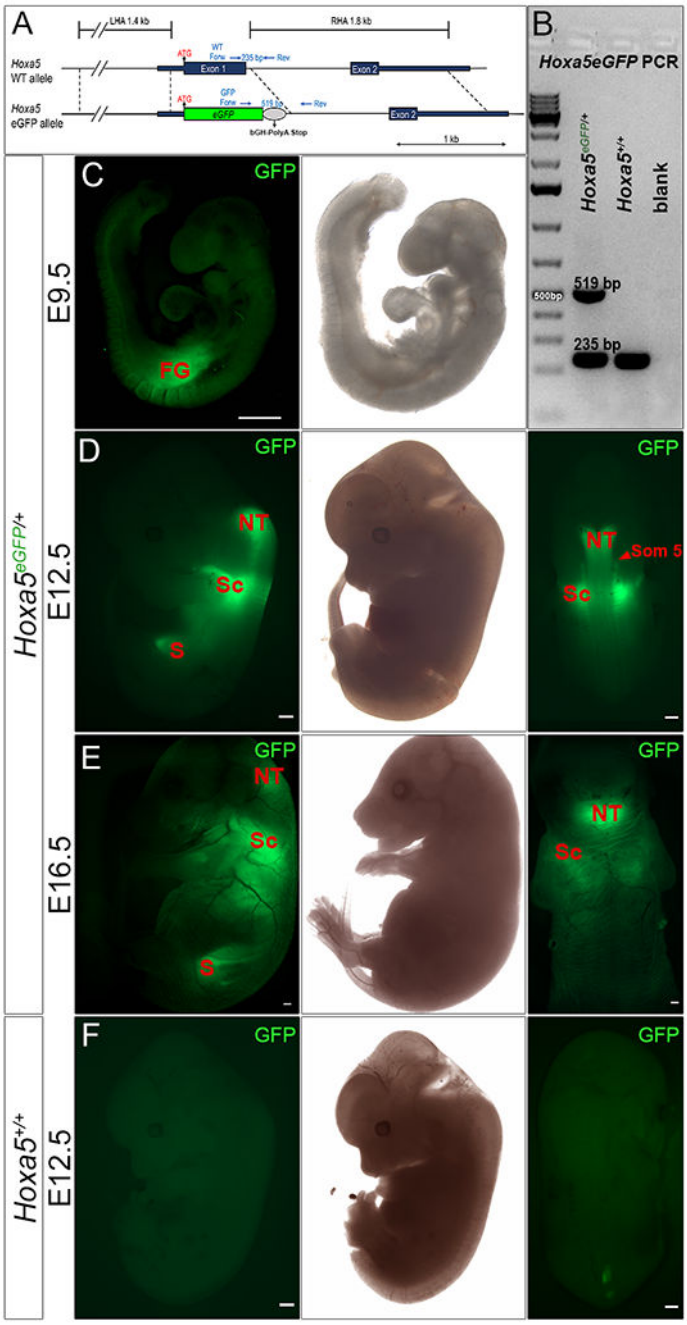


**Figure 1. Generation of the *Hoxa5eGFP* targeted allele in mice and detection in whole-mount embryos.**

**A:** Schematic of the *Hoxa5* WT allele (top) and the *Hoxa5eGFP* allele (bottom). **B**: PCR genotyping validation of *a Hoxa5*$^{eGFP/+}$ and a *Hoxa5*$^{+/+}$ mouse. The *Hoxa5eGFP* allele is identified by the presence of a 519 bp band (top band), the 235 bp band (bottom band) indicates the presence of a WT allele, and blank denotes a PCR reaction without DNA. **C-E:** Embryonic day (E) 9.5, E12.5, and E16.5 *Hoxa5*$^{eGFP/+}$ whole-mount embryos in left lateral view (GFP and brightfield) and dorsal view (GFP). Red arrowhead indicates the anterior

somite boundary of *Hoxa5* expression. **F:** A E12.5 *Hoxa5*$^{+/+}$ (WT) whole-mount embryo in left lateral view and dorsal view. Abbreviations: WT, wild-type; LHA and RHA, left and right homology arm; Forw, forward; Rev, reverse; bGH, bovine growth hormone; FG, foregut; NT, neural tube; Sc, scapula; S, stomach; Som, somite. Scale bars: 500 μm (C-F).

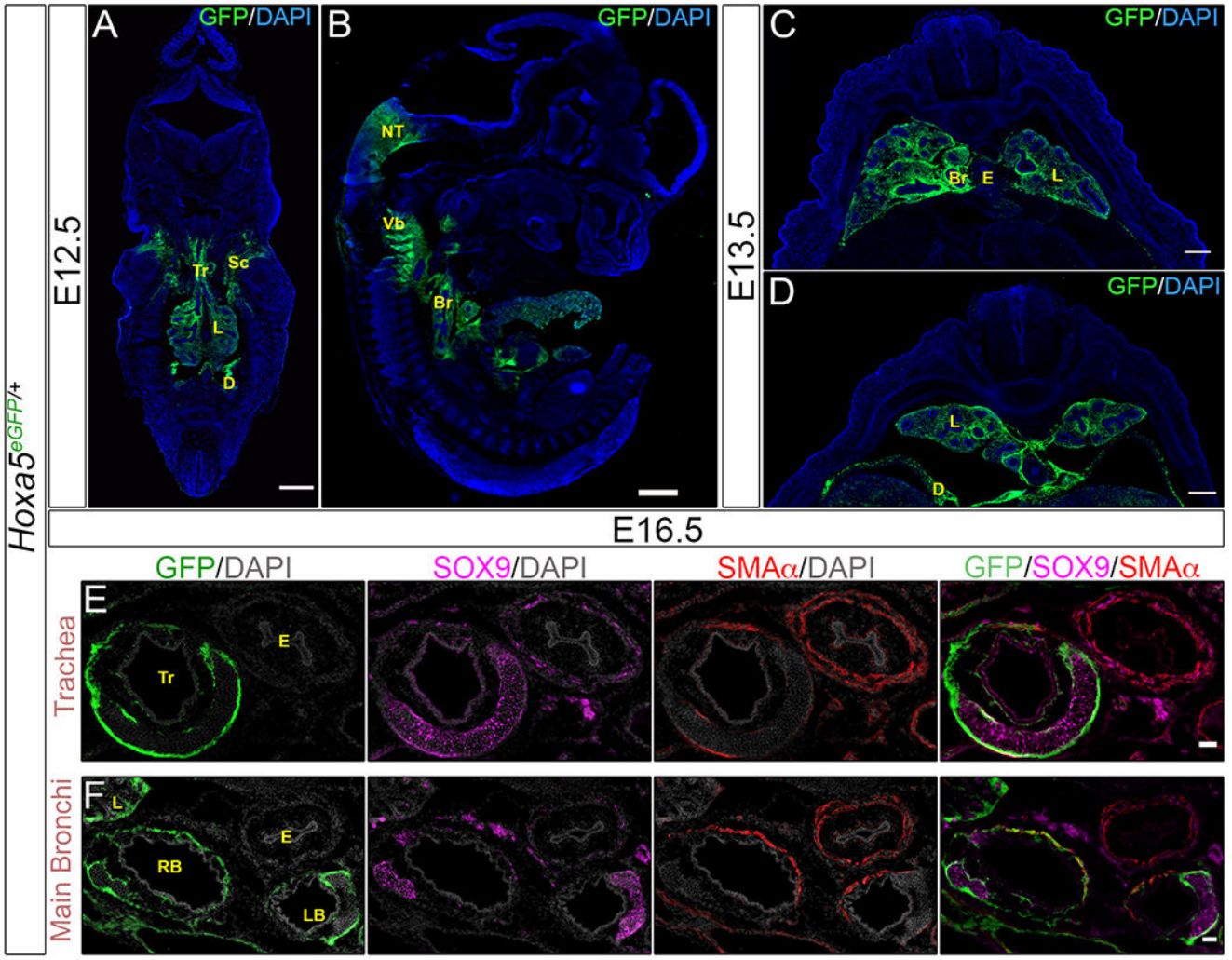


**Figure 2. Mesenchymal Hoxa5eGFP expression in the respiratory system during embryogenesis.**

**A-D:** Frontal **(A)**, sagittal **(B)** and transverse **(C-D)** sections of *Hoxa5*$^{eGFP/+}$ embryos at E12.5 and E13.5. **E-F:** Transverse sections of the trachea **(E)** or main bronchi **(F)** of a *Hoxa5*$^{eGFP/+}$ embryo at E16.5 co-stained with antibodies against SOX9 (magenta) and SMAα (red), and nuclear DAPI staining (grey). Abbreviations: Sc, scapula; Tr, trachea; L, lung; D, diaphragm; NT, neural tube; Vb, vertebrae; E, esophagus; Br, bronchus; RB, right main bronchi; LB, left main bronchi. Scale bars: 500 μm (A-B); 200 μm (C-D); 100 μm (E-F).

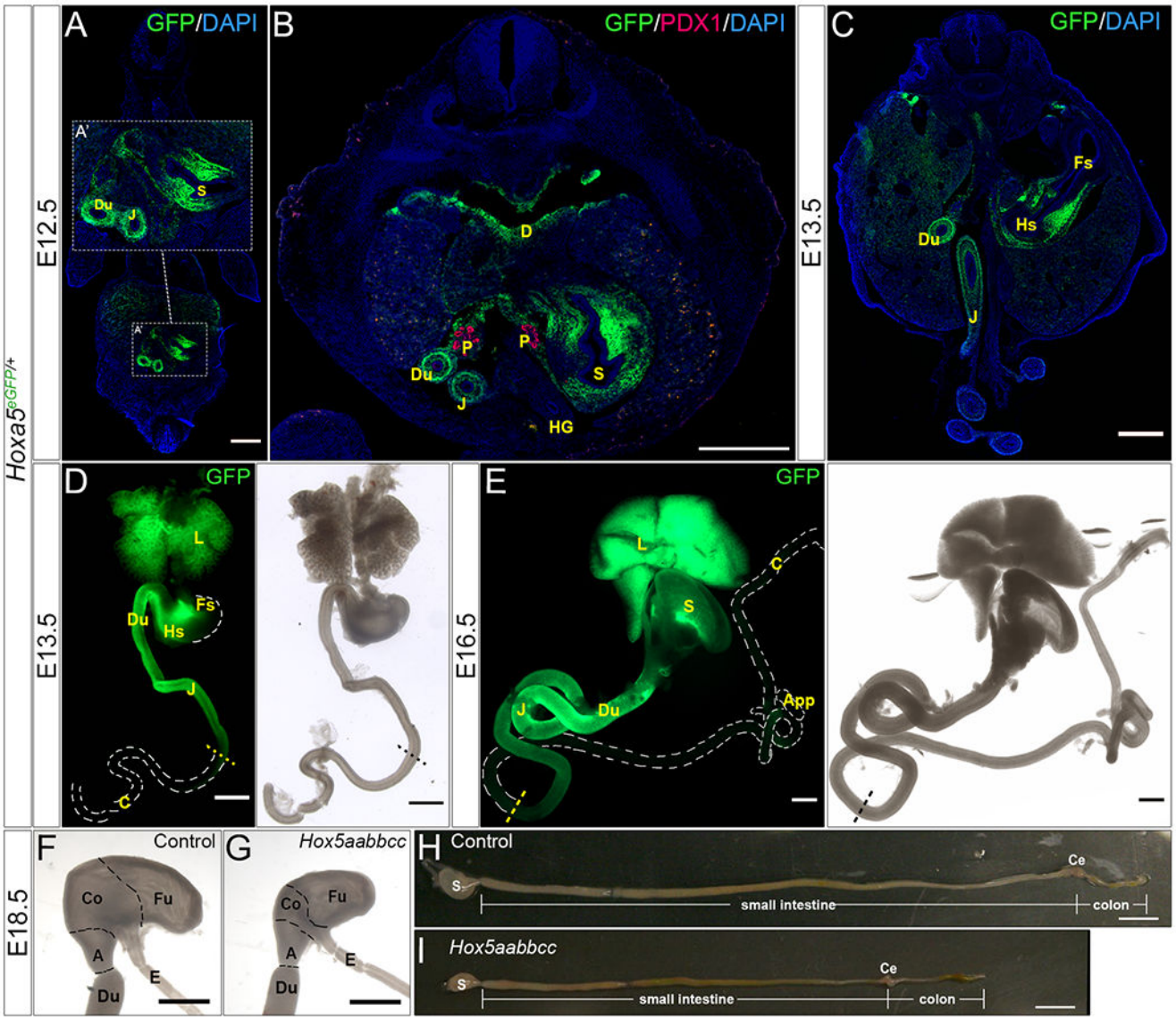


**Figure 3. Hoxa5eGFP localization and *Hox5* null mutant phenotypes in the embryonic gastrointestinal tract.**

**A:** A frontal section of a *Hoxa5*$^{eGFP/+}$ embryo at E12.5. **B:** A transverse section of a *Hoxa5*$^{eGFP/+}$ embryo at E12.5 co-stained with antibody against PDX1 (magenta), a pancreatic epithelial marker. **C:** A transverse section of a *Hoxa5*$^{eGFP/+}$ embryo at E13.5. **A':** A higher magnification of the boxed region in **A**. **D-E:** Whole-mount E13.5 or E16.5 lung and guts in GFP and brightfield view. **F-I:** Whole-mount stomach and guts of control and *Hox5aabbcc* E18.5 embryos in brightfield view. Abbreviations: D, diaphragm; P, pancreas; Du, duodenum; J, jejunum; HG, hindgut; S, stomach; Fs, forestomach; Hs, hindstomach; L, lung; Fu, fundus; Co, corpus; A, antrum; App, appendix; Ce, cecum; C, colon. Scale bars: 500 μm (A-C); 1000 μm (D-E); 2000 μm (F-G); 5000 μm (H-I).

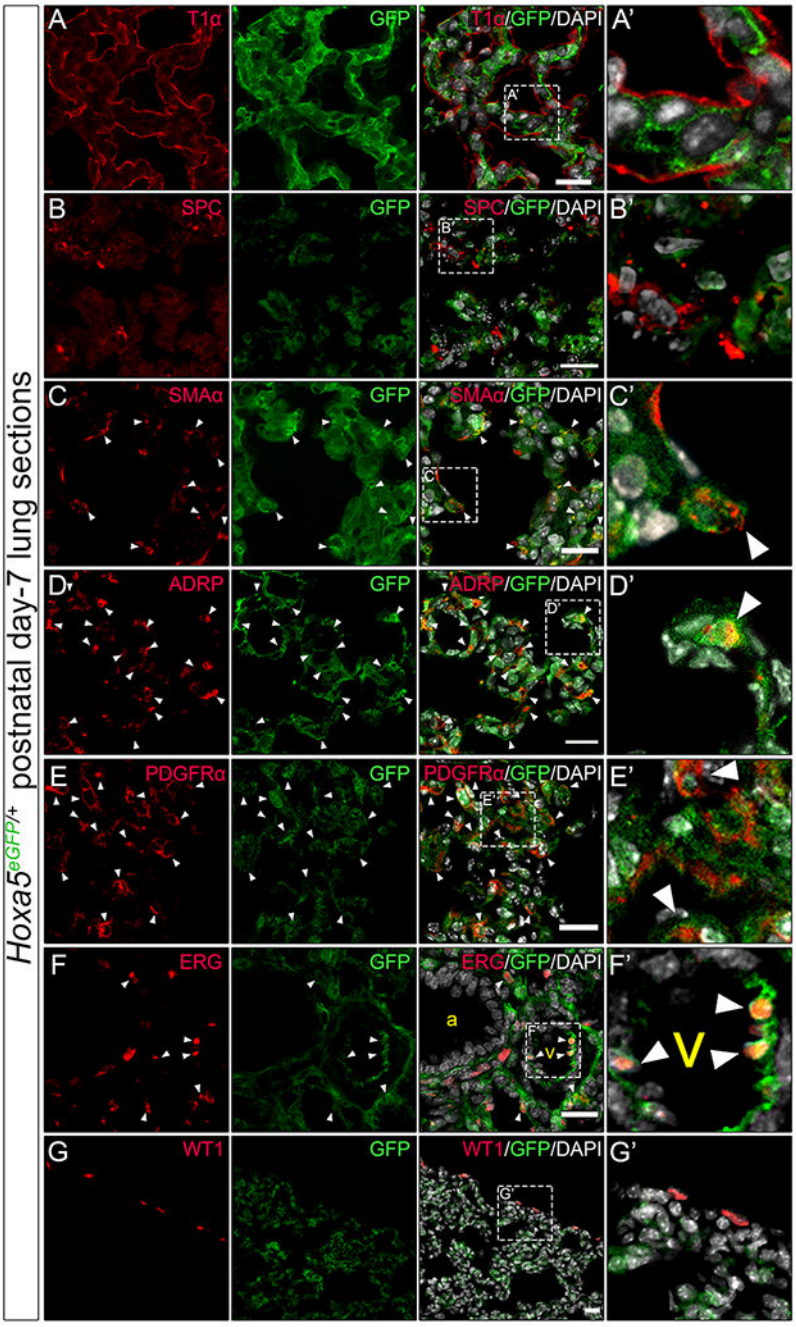


**Figure 4. Hoxa5eGFP-positive cells co-localizing with mesenchymal and endothelial cell markers in the *Hoxa5*$^{eGFP/+}$ postnatal mouse lung.**

**A-G:** Lung cryosections of 7-day-old *Hoxa5*$^{eGFP/+}$ animals were immunostained for GFP, DAPI and T1α **(A),** SPC **(B),** SMAα **(C),** ADRP **(D)**, PDGFRα **(E)**, ERG **(F)**, and WT1 **(G).** In each figure, the red channel represents a cell marker antibody, the green channel represents Hoxa5eGFP+ cells, and the grey channel marks nuclear DAPI staining. **A'-G':** Higher magnification of boxed regions in **A-G**. White arrowheads in **C-F** and **C'-F'** indicate double-positive cells. Abbreviations: a, airway; v, vascular. Scale bars: 20 μm (A-G).

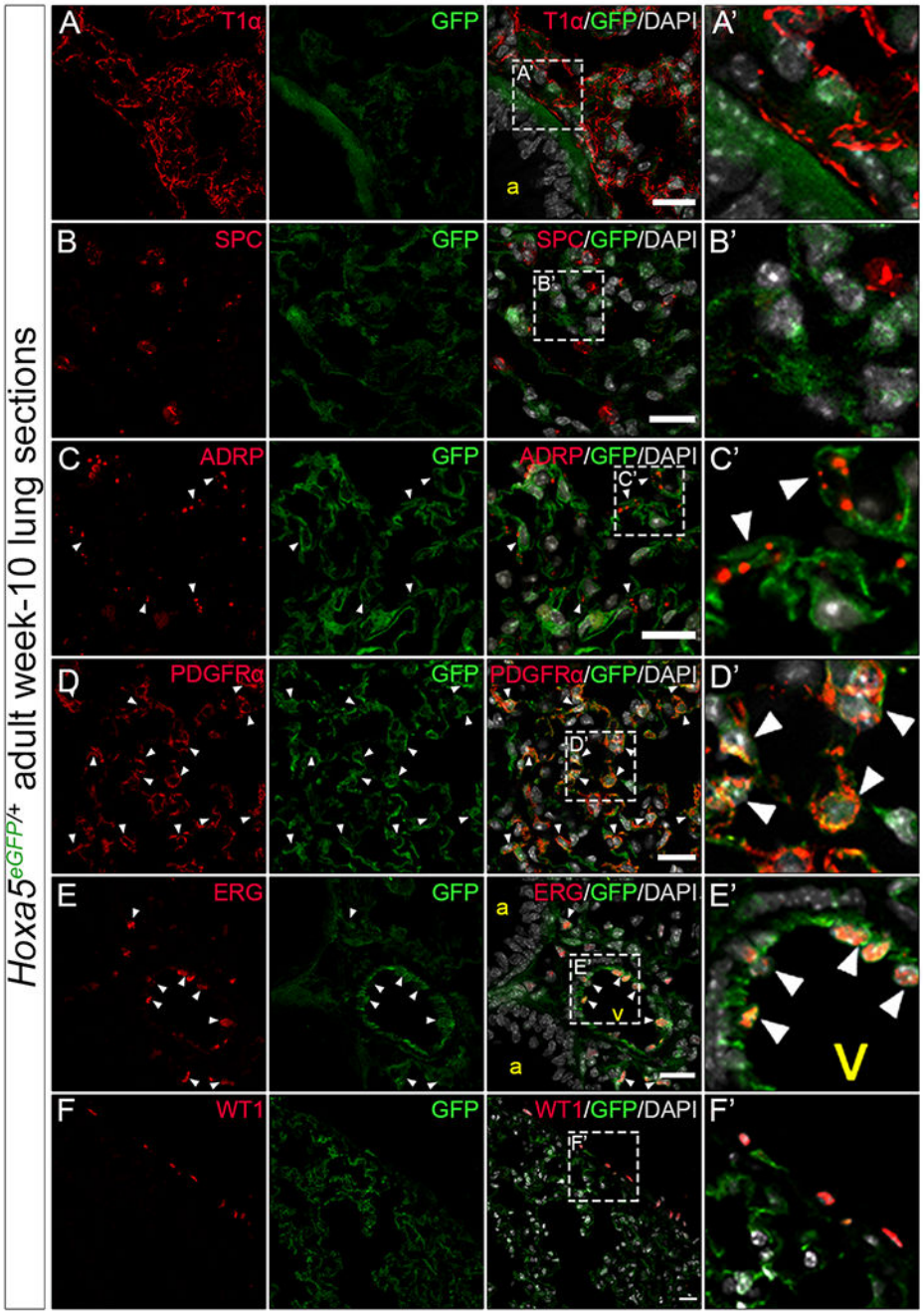


**Figure 5. Expression of Hoxa5eGFP in mouse lungs continues through the adult stage.**

**A-F:** Lung cryosections of 10-week-old *Hoxa5*$^{eGFP/+}$ animals were immunostained for GFP, DAPI and T1α **(A),** SPC **(B),** ADRP **(C)**, PDGFRα **(D)**, ERG **(E)**, and WT1 **(F).** In each figure, the red channel represents a cell marker antibody, the green channel represents Hoxa5eGFP+ cells, and the grey channel marks nuclear DAPI staining. **A'-F':** Higher magnification of boxed regions in **A-F**. White arrowheads in **C-E** and **C'-E'** indicate double-positive cells. Abbreviations: a, airway; v, vascular. Scale bars: 20 μm (A-F).

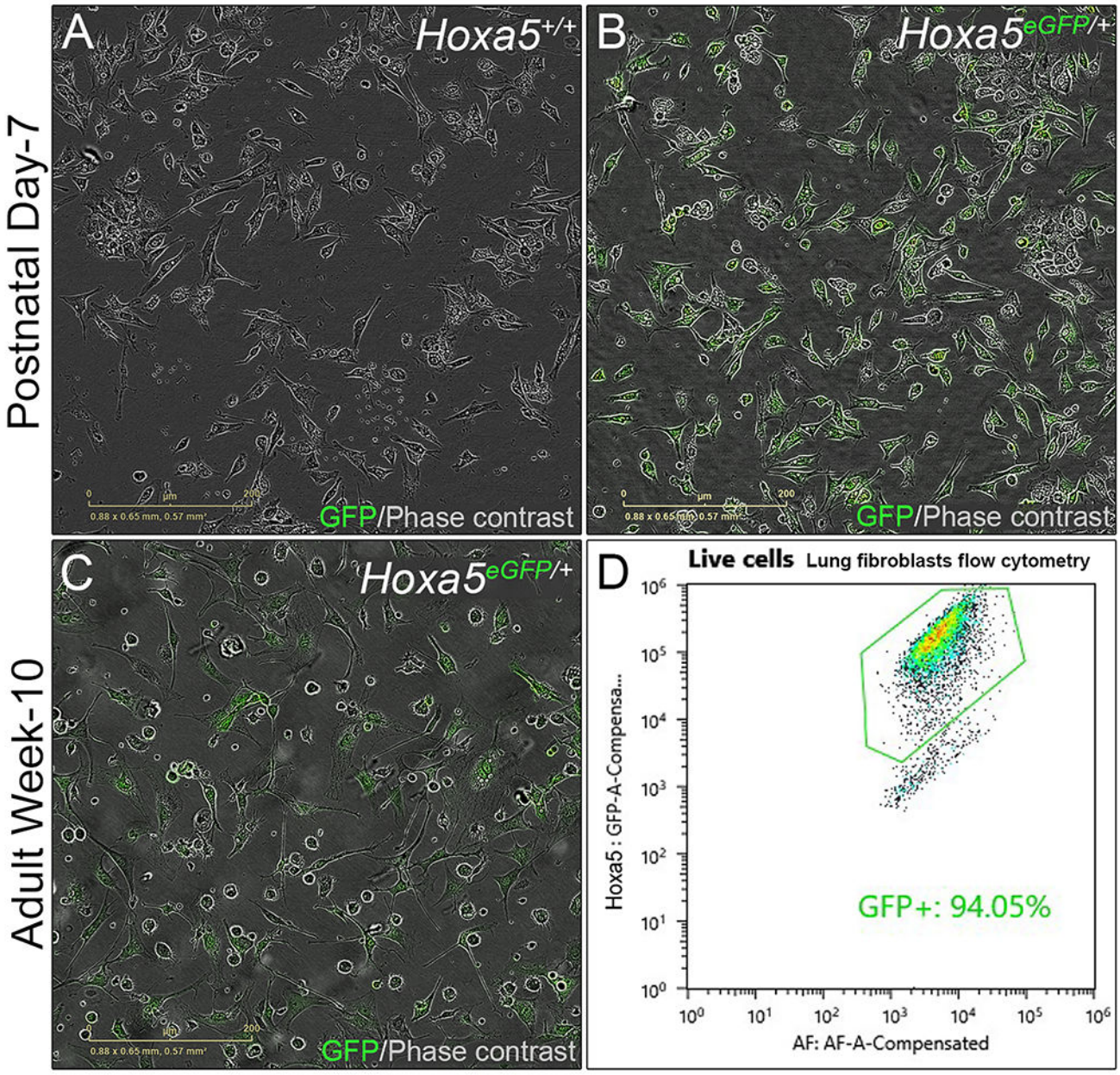


**Figure 6. Hoxa5eGFP expression in lung fibroblasts *in vitro* and via flow cytometry analysis.**

**A-C:** GFP and phase contrast field of lung fibroblasts isolated from postnatal *Hoxa5*$^{+/+}$ **(A)**, postnatal *Hoxa5* $^{eGFP/+}$ **(B)**, and adult *Hoxa5*$^{eGFP/+}$ **(C)** mice in 6-well plates at passage 0. **D:** Flow cytometry dot plots demonstrate that 94.05% of the isolated 10-week-old adult lung fibroblasts are Hoxa5eGFP-positive at passage 8. Abbreviation: AF, autofluorescence. Scale bars: 200 μm (A-C).

**Table 1.**

List of antibodies used for immunostaining

| Antibody | Host species | Conjugate | Dilution | Supplier | Catalogue number |
|---|---|---|---|---|---|
| ADRP | Rabbit | N/A | 1:200 | Abcam | ab78920 |
| ERG | Rabbit | N/A | 1:200 | Abcam | ab92513 |
| GFP | Chicken | N/A | 1:300 | Abcam | ab13970 |
| PDGFRα | Rabbit | N/A | 1:50 | Cell Signaling | 3174S |
| PDX1 | Guinea Pig | N/A | 1:200 | Abcam | ab47308 |
| SMAα | Mouse | Cy3 | 1:500 | Sigma | C6198 |
| SOX9 | Rabbit | N/A | 1:500 | Sigma | AB5535 |
| SPC | Rabbit | N/A | 1:500 | Seven Hills | WRAB-9337 |
| T1α | Syrian Hamster | N/A | 1:100 | DSHB | 8.1.1 |
| WT1 | Rabbit | N/A | 1:200 | Invitrogen | MA5-32215 |